Vol. 691: 29–40, 2022
https://doi.org/10.3354/meps14072

MARINE ECOLOGY PROGRESS SERIES
Mar Ecol Prog Ser

Published June 16

Discovery and dynamics of a cryptic marine copepod–parasite interaction

Eric C. Orenstein[1,4,*], Erik Saberski[1], Christian Briseño-Avena[2,3]

[1]Scripps Institution of Oceanography, University of California, San Diego, CA 92093, USA
[2]Department of Environmental and Ocean Sciences, University of San Diego, CA 92110, USA
[3]Department of Biology and Marine Biology, University of North Carolina, Wilmington, NC 28403, USA

[4]*Present address:* Monterey Bay Aquarium Research Institute, Monterey, CA 95039, USA

ABSTRACT: Parasitism is increasingly recognized as a critical element of ecosystem dynamics but remains understudied due to observational limitations, especially in rapidly fluctuating marine plankton populations. We combined 3 new techniques — *in situ* imaging microscopy, automated classification, and empirical dynamic modeling — to quantify interactions between *Oithona* spp. and the rhizarian parasite *Paradinium* spp. at hourly resolution for over 1 yr in the Southern California Bight. We investigate the time scales, host population effects, and potential environmental drivers of infection. Our study suggests that *Paradinium* spp. is consistently present in the local copepod population at low levels throughout the year and that the parasite exerts control on the host population on a 22–23 d lag — a delay consistent with known *Oithona* spp. generation times. The interaction strength was pronounced at higher temperatures, suggesting that *Paradinium* spp. will have a significant role in local ecosystem dynamics as surface ocean temperatures rise.

KEY WORDS: Parasitic interaction · Population control · Marine copepods · *Oithona* · Rhizarian · *Paradinium* · *In situ* microscopy · Time series

1. INTRODUCTION

Parasites are a consistent feature of all ecosystems, account for about 40% of global biodiversity, and have a demonstrable impact on food web dynamics (Lafferty et al. 2006, Dobson et al. 2008, Lima-Mendez et al. 2015). Parasitic interactions, however, are often cryptic and challenging to observe, particularly in pelagic marine ecosystems (Harvell et al. 1999, McCallum et al. 2004). The difficulties associated with studying parasites in the open ocean have led to parasitism being an overlooked interaction in marine food webs (Shields 2019). Modeling studies of ocean ecosystems typically focus on quantifying controls on planktonic populations as top-down, via predation, or bottom-up, via food abundance (Ohman 1986, Sabatini & Kiørboe 1994, Ji et al. 2013). Short-term or opportunistic observational studies have noted a significant parasitic effect on the survival and fecundity of marine plankton (Ianora et al. 1987, Fields et al. 2015), yet the lack of long-term observational data has stymied efforts to assess the impact of parasites on population dynamics (Johnson et al. 2009).

The impact of parasitism on marine zooplankton populations is particularly understudied (Sommer et al. 2012, Skovgaard 2014, Shields 2019). Copepods play a crucial role in all aquatic ecosystems and biological carbon cycling. They are arguably the most numerous metazoans on the planet and are a major link between carbon fixed by photosynthetic phytoplankton and higher trophic levels (Kiørboe 1997, Legendre & Rivkin 2002, Turner 2004). Copepod abundances are known to vary with both environmental factors, such as physical forcing and biogeo-

*Corresponding author: eorenstein@mbari.org

Publisher: Inter-Research · www.int-res.com

chemical cycling, and biotic interactions, typically viewed through the lens of trophic interactions (Verity & Smetacek 1996). Although the existence of parasites of marine zooplankton has been extensively documented, and much effort devoted to their taxonomy and systematics, the ubiquity of parasites, their ecological role, and their effect on energy transfer remains largely unknown (Ho & Perkins 1985, Théodoridès 1989, Skovgaard & Saiz 2006). Recent advances in genetic techniques have confirmed the widespread and consistent distribution of parasites associated with marine plankton (Lima-Mendez et al. 2015, Guidi et al. 2016).

Tracking parasitic infections at high enough spatiotemporal resolution to assess the effect on a host population is challenging due to limitations associated with traditional net or bottle-based sampling techniques. Moreover, standard chemical preservation or improper handling of samples can make the identification of parasites intractable or impossible, rendering most historical samples difficult to analyze (Ianora et al. 1987, Skovgaard & Saiz 2006, Shields 2017). Expanding the coverage of such monitoring is inhibited by its labor-intensive nature; the work entails countless hours of expert sorting of net samples, taxonomic identification, and maintenance of cultures (Benfield et al. 2007, MacLeod et al. 2010).

In this study, we tracked temporal variability in the presence of the ectoparasitic phase of the genus *Paradinium* on the cosmopolitan cyclopoid copepod genus *Oithona* off the coast of Southern California, one of the most studied planktonic ecosystems in the world, marking the first observation of the parasite in the Northern Pacific. *Paradinium* spp. is believed to be widespread in coastal waters but is difficult to observe due to the transient nature of the external gonosphere life stage. The mass only remains attached to the copepod on time scales of minutes to hours and can be dislodged when sampling with a net or lost in chemical fixation (Shields 1994, Skovgaard & Saiz 2006, Ward et al. 2018). The infection can also reach considerable prevalence, with documented rates of up to 35% of the host population in Mediterranean waters (Chatton & Soyer 1973). The parasite's effect on its host population remains unknown.

We quantified the interaction at hourly resolution using a combination of 3 recently developed observational and analytic techniques: *in situ* microscopic imaging, automated image classification with convolutional neural networks (CNNs), and time series analysis with empirical dynamic modeling (EDM) (Sugihara et al. 2012, LeCun et al. 2015, Deyle et al. 2016, Orenstein et al. 2020b). Using imagery collected by the Scripps Plankton Camera (SPC), we generated a year-long, hourly resolved time series tracking the short-term end-stage of *Paradinium* spp. infecting *Oithona* spp. We then evaluated the time series in the context of coincident environmental parameters to assess the influence of the parasite on the copepod host population. Given the ecological significance and global distribution of *Oithona* spp., we posit that the parasitic infection is a common and important element of many coastal ecosystems. Our work suggests that real-time monitoring coupled with robust time series analyses is a viable approach to quantifying the effect of ectoparasites on zooplankton populations and evaluating the role of parasites in the pelagic food web.

2. MATERIALS AND METHODS

We combined 3 distinct techniques to identify relevant time scales of *Paradinium* spp. infection and control of *Oithona* spp. populations in the Southern California Bight (SCB). Images were collected by the SPC, and a deep neural network was trained to classify the images and generate a time series. Dynamic modeling methods were used to analyze the resulting data to quantify the relationship between the parasite and its copepod host.

2.1. Study system

2.1.1. Physical environment

All data were collected at the Ellen Scripps Memorial Pier at the Scripps Institution of Oceanography in La Jolla, California. The pier deck extends approximately 250 m offshore into nearshore waters. The environment sampled at the pier is strongly influenced by tides, atmospheric interactions, and coastal processes such as shoaling internal waves (Pineda 1991, Morgan et al. 2017, Sinnett et al. 2018). The SPC has been deployed on the southeast corner of the pier deck at a tide-dependent average depth of 3 m since March 2015. The images for the present study were collected between March 2015 and April 2016.

The physical and biological environment in the Southern California Current System is generally regulated by surface heat flux, horizontal advection, wind stress, and upwelling (Huyer 1983, Beardsley et al. 1998, Bograd et al. 2001). The system is modulated by decadal-scale features such as the El Niño–Southern Oscillation and the North Pacific Gyre

Oscillation (Lynn & Bograd 2002, Di Lorenzo et al. 2008). The study year, however, was climatologically unique, characterized by a persistent warm-water anomaly known as 'the Blob' (Cavole et al. 2016). In the SCB, the Blob reduced surface heat flux, leading to increased stratification that altered historic patterns of upwelling and downwelling along the coast (Jacox et al. 2016). The increased thermal stratification also caused a reduction in vertical mixing that reduced the nutrient flux to surface waters (Zaba & Rudnick 2016). At the Scripps Pier in particular, 199 d during the year-long study period qualified as being anomalously warm compared to historical water temperature records (Fumo et al. 2020).

2.1.2. Host

Oithona spp. is a cosmopolitan cyclopoid copepod genus that is common in coastal marine environments. There are 3 species of *Oithona* typically found in the SCB and at Scripps Pier in particular: *O. nana*, *O. setigera*, and *O. similis*. *O. nana* is easy to differentiate from the others based on average body size: the typical *O. nana* individual is approximately 1 mm smaller than the other species. *O. setigera* and *O. similis* are challenging to distinguish in SPC images since their morphological differences approach the pixel-level resolution of the instrument. We thus refer to the host as *Oithona* spp., noting that *O. similis* is by far the most frequent and abundant species sampled at the Scripps Pier (Nishida 1985).

2.1.3. Parasite

Paradinium is currently a monotypic rhizarian genus with the extant species *P. poucheti* Chatton, 1910. There are 3 recognized *Paradinium* species parasitizing copepods: *P. poucheti* associated with *Acartia cluasii*, *A. longiremis*, and *O. similis* (Chatton 1910); *P. mesnili* parasitizing *Triconia conifera* (Chatton & Soyer 1973); and *P. cauleryi* found with *Ocaea media* (Chatton & Soyer 1973). A fourth unknown species of *Paradinium* is associated with *Euterpina acutifrons* (Skovgaard & Daugbjerg 2008). Recent molecular studies have confirmed *Paradinium*'s association with at least 2 copepods via small subunit (SSU) rRNA analysis: *P. poucheti* from *O. similis* (PaOi01) and an undescribed *Paradinium* sp. from *E. acutifrons* (PaEu41) (Skovgaard & Daugbjerg 2008). *P. poucheti* is the most well-studied of the 4 known species and has been identified in amplified eDNA samples taken in Florida, Borneo, UK, Italy, Norway, and South Africa (Ward et al. 2018).

P. poucheti is a parasitic rhizarian that grows in the host's haemocoel, migrates into the digestive tract, is expelled through the anus, and finally attaches as a cell mass called a gonosphere to the host's anal somite (Chatton 1910). After several hours, flagellated spores form in, and subsequently emerge from, the gonosphere, possibly representing the parasite's infectious stage (Skovgaard & Daugbjerg 2008). The gonosphere remains attached to the host for a matter of hours (see Fig. 1b). *P. poucheti* is believed to be a parasitic castrator, preferentially targeting females and destroying the gonads as it grows (Shields 1994, Lafferty & Kuris 2009). While no complete life cycle has been documented for *P. poucheti*, the organism is thought to take about 4 wk from infection to expulsion of flagellated, free-swimming bodonisphores (Shields 1994).

To our knowledge, there are no published reports of *Paradinium* in the North Pacific (Ward et al. 2018). However, a single SSU rRNA sequence of an uncultured marine eukaryote clone collected along the Southern California coast matched 96% of the positions of 2 complete sequences of corroborated *P. poucheti* isolates from the NW Mediterranean (Worden 2006, Skovgaard & Daugbjerg 2008). We did not have the resources in the context of this work to collect our own genetic samples.

The ephemeral gonospheres observed in this study are likely the end stage of *Paradinium*'s life cycle based on the highly specific copepod–parasite association, mode of attachment to the host during the parasite's external life phase, and macroscopic morphology of the gonosphere. Without laboratory-based morphological measurements or molecular data, we cannot positively identify the parasite to the species level. We conservatively report our observation as *Paradinium* spp. until further evidence can confirm the parasite's taxonomic position.

2.2. *In situ* microscopy and environmental data

The SPC is an *in situ* dark-field microscope designed as a complement to the ongoing Scripps Pier plankton time series maintained by the Southern California Coastal Ocean Observing System (SCCOOS) through the Harmful Algal Bloom Monitoring and Alert Network (Kim et al. 2009, Orenstein et al. 2020b). The SPC consists of 2 housings: one contains an LED light source and collimating optics; the other, a machine vision camera, embedded computer, and

power supply. The sample volume between the housings is undisturbed fluid — the system uses no nets, filters, or pumps — and thus samples only the ambient plankton population. The system captures 8 frames s^{-1} and, using real-time object detection, extracts regions of interest (ROIs). The SPC logs thousands to millions of ROIs d^{-1} depending on the ambient density of objects in the water. The data presented in this paper were collected by an SPC fitted with a 0.5× microscope objective for observing zooplankton and large phytoplankton.

Coincident environmental data were recorded by the SCCOOS automated shore station package — an instrument attached to an adjacent pier piling at approximately the same depth as the SPC. Data acquired by the environmental sensors were downloaded from NOAA's Environmental Research Division Data Access Program. The physical data were quality controlled by SCCOOS software according to the Integrated Ocean Observing System's standards.

The data collected by the SPC have a number of important technical limitations related to resolution and sample volume. The camera, fitted with a 0.5× magnification objective, yields 7.4 µm $pixel^{-1}$ in object space — 32 line pairs mm^{-1} at 30% contrast on a USAF 1951 resolution target — and captures approximately 3 ml of fluid $frame^{-1}$. The pixel resolution is sufficient to identify *Oithona* spp. and distinguish the egg sacs from the ephemeral ectoparastic phase of *Paradinium* spp., but not to sort males and females. The volume per frame is size-dependent — larger objects blur out over larger distances and thus have a larger effective sample volume. Furthermore, the imaging system only captures the ephemeral ectoparasitic phase of *Paradinium* spp. and does not allow us to determine if a copepod imaged without an attached gonosphere is infected or not. We are therefore careful in the subsequent analyses to present estimated parasite prevalence in the population rather than prevalence as traditionally stated in parasitology studies (Margolis et al. 1982, Bush et al. 1997). Likewise, we present our findings in terms of relative, not absolute, abundance. Thus, subsequent results should be understood as descriptive of patterns and magnitudes rather than absolute changes in the population during the sample period.

2.3. Image classification

The SPC images were sorted into 3 classes of interest: *Oithona* spp., *Oithona* spp. with *Paradinium* spp. gonosphere, and *Oithona* spp. with egg sacs (Fig. 1). *Oithona* spp. is readily identifiable from other copepod genera in the SPC images due to the distinctive, approximate 1:1 ratio between the prosome and urosome length. Egg sacs and gonospheres are easily distinguishable due to differences in shape and color. The egg sacs are elongated, translucent, and attached in pairs to the genital somite. The gonospheres are ovular, opaque brown, and appear to be trailing the host's urosome. All other images were classified as 'other', a catch-all class for objects not relevant to the present study. We leveraged recent advances in machine learning and pattern recognition to separate 10s of millions of unannotated ROIs. Broadly speaking, we used a supervised machine learning approach — a procedure in which an expert

Fig. 1. Example images from the Scripps Plankton Camera drawn from the classes of interest. (a) *Oithona* spp.; (b) *Oithona* spp. with ectoparasite phase (gonosphere), presumed to be *Paradinium* spp. (arrowhead); (c) *Oithona* spp. ovigerous females with egg sacs (arrowhead). Note the variety of body angles relative to the image plane and pose of appendages. These images are notably clean compared to the entire training set for the automated classifier; human annotators selected images of many poses if they were 80% confident of their label

human annotator sorts images that are then used to train a computer classifier for later use on new data.

2.3.1. Manual annotation

Manual annotation efforts for this study began in 2015 when *Paradinium* spp. gonospheres were first observed on *Oithona* spp. in the SPC data. Using a custom web-based labeling interface, ROIs were filtered by major axis length and constrained to 0.5–2.5 mm based on well-established size ranges for *Oithona* spp. and the camera geometry. In total, a human expert annotated 643 018 ROIs in that size range from 58 randomly selected days between 12 March and 31 July 2015. In those days, 10 645 ROIs belonged to *Oithona* spp., 1660 were *Oithona* spp. ovigerous females, and 1013 were *Oithona* spp. with *Paradinium* spp. gonosphere.

2.3.2. Automated classification

The manually labeled images were used to train a deep CNN, a machine learning framework that learns directly from images rather than features defined by an engineer (LeCun et al. 2015). A version of the AlexNet architecture consisting of 5 convolutional and 3 fully connected layers, originally trained on the ImageNet natural image database, was fine-tuned with the labeled SPC data using the Caffe deep learning library (Krizhevsky et al. 2012). Fine-tuning is a common CNN training procedure that initializes model weights from a network developed for a different task rather than from random (Yosinski et al. 2014). Recent work has demonstrated that networks fine-tuned with plankton data outperform those trained from scratch when limited training data are available (Orenstein & Beijbom 2017). The training distribution was forced to be uniform by subsampling all 4 classes (the 3 classes of interest and 'other') to contain only 1000 images each. This procedure biases the classifier to be more sensitive to the classes of interest (González et al. 2017, Orenstein et al. 2020a). In effect, we trained the classifier to have a low false omission rate at the cost of a relatively high false detection rate. Moreover, the artificially uniform training distribution is more robust to data set shift — the variability in classifier performance as a function of changes in the underlying population (Moreno-Torres et al. 2012).

AlexNet was fine-tuned for 25 epochs with a learning rate of 0.0002 on an NVIDIA Tesla K40 GPU. The resulting model achieved an accuracy of 89% on an independent in-distribution test set composed of a random subset of 15% of the training data. The classifier was then further evaluated on all unlabeled data collected between March and September 2015. All ROIs labeled as one of the 3 classes of interest in that time frame were validated by a human expert to assess the classifier performance. Errors were tallied on a class-by-class basis in a binary manner and used to compute the false detection (FDR) and false omission rates (FOR):

$$\mathrm{FDR} = \frac{\sum \mathrm{FP}}{\sum \mathrm{FP} + \sum \mathrm{TP}} \quad (1)$$

and

$$\mathrm{FOR} = \frac{\sum \mathrm{FN}}{\sum \mathrm{FN} + \sum \mathrm{TN}} \quad (2)$$

where FP and TP denote false and true positive respectively. Likewise, TN and FN represent true and false negatives. These metrics allow users to judge the performance of a system as a function only of the labels returned in a single class (Genovese & Wasserman 2002, Storey 2003). This is helpful in the current case where the number of true negatives — ROIs in the 'other' class — is far greater than those in the classes of interest (Orenstein et al. 2020a).

The evaluation demonstrated the model had a FDR of 0.08 on *Oithona* spp. and 0.23 on *Oithona* spp. with *Paradinium* spp. gonosphere. The computer had the most trouble with the *Oithona* spp. ovigerous female class, returning a FDR of 0.32. The system did not, however, return many false negatives; the human expert examined approximately 30 000 randomly selected ROIs that the computer placed in the 'other' category and only discovered 4 false negatives (FOR $\ll$ 0.01). These error rates reflect that the classifier is prone to overestimating the classes of interest and that the resulting counts should be understood as a maximum estimate. This underscores that the classifier output should be interpreted as indicative of community patterns and not absolute, volumetrically exact changes in the population.

2.4. EDM

The CNN counts were binned at hourly resolution and used to generate a daily averaged time series of *Oithona* spp., *Oithona* with egg sacs, and *Oithona* with an attached *Paradinium* spp. gonosphere. These counts were smoothed with a 24 h running median filter (see Fig. 2a). The resulting count data were used to assess the apparent relative percentage of infected and ovigerous *Oithona* spp. based on the SPC

data. The percentage was computed at each time point as the number in the class over the total number of identified *Oithona* spp. (see Fig. 2b).

Using convergent cross-mapping (CCM), we sought to identify non-linear, causal relationships between *Paradinium* spp. and *Oithona* spp. from the time series generated by the CNN (Sugihara et al. 2012). CCM tests for causation by measuring how well historical values of one time series can predict states of the other. The predictions are computed by time-lag embedding 2 time series to produce sets of n-dimensional points (x_t, x_{t-1}, … x_{t-n+1}) at each time t for both signals. Every n-dimensional point represents a unique state of the system, a so-called state space reconstruction. If similar states of one time series map to similar states of another, the 2 are dynamically coupled. CCM can thus identify ecosystem coupling and associated temporal lags directly from data with only minimal assumptions (Ye et al. 2015).

Here, we calculated CCM in 7 dimensions (time-lags of 0–6 d), with delays ranging from 0–42 d. We measured CCM strength as the accuracy (Pearson's correlation) of mapped, or predicted, values on the target attractor from the library attractor. Because each point in the reconstructed attractor represents 7 consecutive days, the delay of the interaction measured by CCM is ambiguous within a 7 d window. To account for the ambiguity, we averaged the CCM strength across 7 d to generate an 'interaction profile' (strength of interactions vs. delay; see Fig. 3a) that is normalized to the embedding dimension (Saberski et al. 2021).

Although CCM identifies the presence and relative strength of non-linear, dynamic interactions, the procedure does not directly quantify the sign of such interactions. We identified the sign of this interaction with *S*-map coefficients (Sugihara 1994, Deyle et al. 2016, Ushio et al. 2018). *S*-maps use local linear maps along an attractor to predict future values. Each local map quantifies the partial derivatives between all variables in the embedding and the target time series at a specific point in time. *S*-maps are sensitive to the set of variables and delays used; relationships quantified with one embedding may change when recalculated in a different embedding (Deyle et al. 2016). Ideally, one would use an embedding that captures all of the causal variables in the system and thus makes perfect predictions, but in most real-world systems such data are not realistically available.

Instead of relying on one specific partial embedding, we generated 100 random embeddings — combinations of variables with lags — of sea surface temperature (with a lag of 0–4 d), *Oithona* spp. relative abundance, *Oithona* spp. ovigerous females (with a lag of 0–20 d), and *Oithona* with ectoparasite (with a lag of 23–26 d). This suite of lags allowed us to find relationships that were not specific to any one embedding. A 14 d moving average was applied to the *Oithona* with parasite time series to reduce noise, and the lag between 23–26 d was chosen based on the peak CCM strength shown in the interaction profile (see Fig. 3a).

3. RESULTS

3.1. Parasite–host observations

The CNN-based counts of the classes of interest were binned at hourly resolution and smoothed with a 24 h running median filter (Fig. 2a). The resulting count data were used to estimate the prevalence of infected and ovigerous *Oithona* spp. based on the SPC imagery. The estimated prevalence was computed at each time point as the number in the class over the total number of identified *Oithona* spp. (Fig. 2b). *Paradinium* spp., as assessed by the visible transient gonosphere on the *Oithona* spp., was present throughout the entire year of data collected by the SPC. The average estimated prevalence of *Paradinium* spp. during the year of study was 9.5%, ranging from 0% to a high of 49% on 19 Jan 2016. The variability in the estimated prevalence is a function of both the host–parasite association and environmental factors. Qualitatively, the *Paradinium* spp. signal appears out of phase with the presence of ovigerous *Oithona* spp., which is consistent with the suggestion that *Paradinium* spp. is a parasitic castrator.

3.2. Population dynamics

There was no strong linear correlation between the counts of apparently uninfected *Oithona* spp. and those with an attached external gonosphere. The lack of linear correlation suggests that if *Paradinium* spp. does exert a control on the *Oithona* spp. population, the coupling is likely state-dependent, or non-linear. The interaction profile generated from the 7-dimensional CCM between *Paradinium* spp. and *Oithona* spp. signals revealed that the parasite had a causal influence on host abundance with a peak effect at 23 d (Fig. 3a). Further, we found that elevated counts of the parasite were consistent with a decline in the number of ovigerous females observed by the SPC with a slightly longer delay of 26 d (Fig. 3a). The

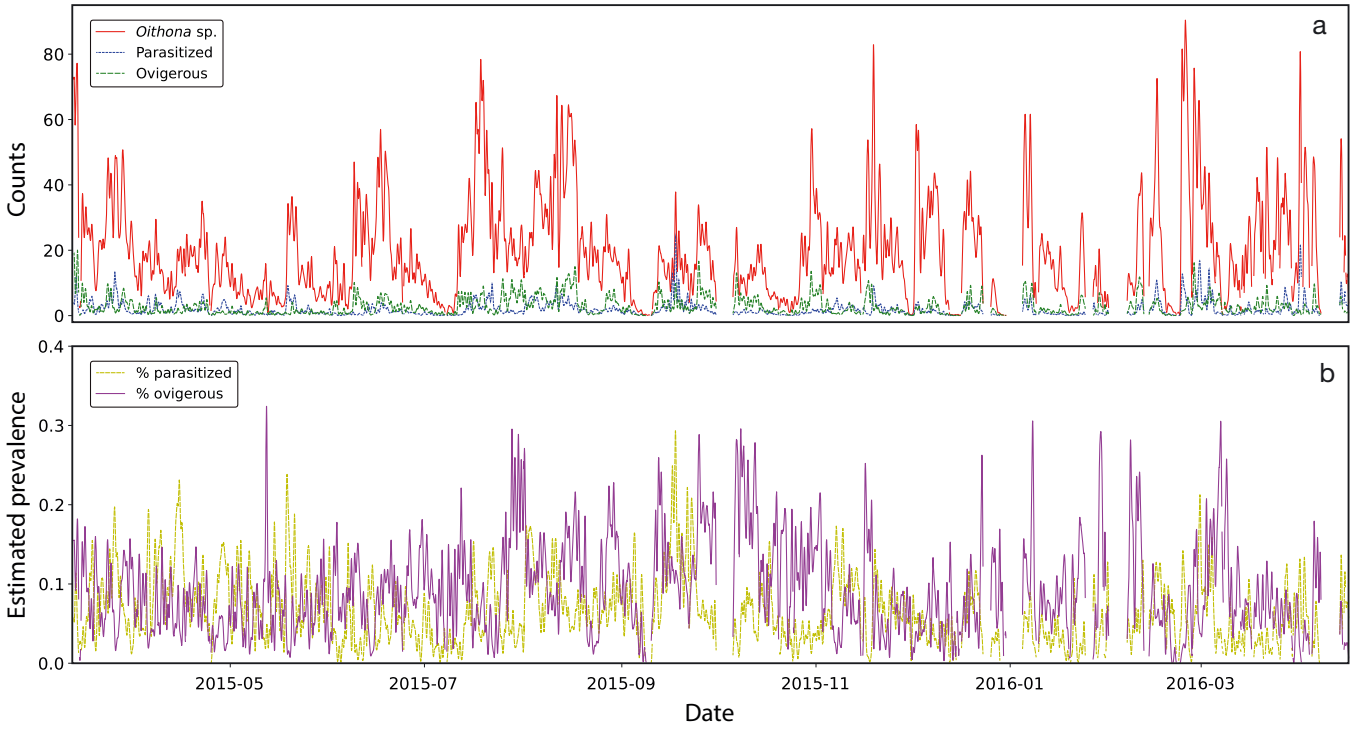

Fig. 2. Time series of *Oithona* spp. tracked with the Scripps Plankton Camera (SPC) between March 2015 and April 2016. The image labels used in these plots are generated by the automated classifier. Data before September 2015 has been fully validated by a human annotator. (a) Count data from the SPC smoothed with a 24 h running mean filter. The number of *Oithona* spp. seen by the SPC is typically much higher than either parasitized or ovigerous individuals. (b) Estimated prevalence of parasitized and ovigerous *Oithona* spp. Percentages are computed by dividing each signal by the total number of *Oithona* spp. in each hourly interval

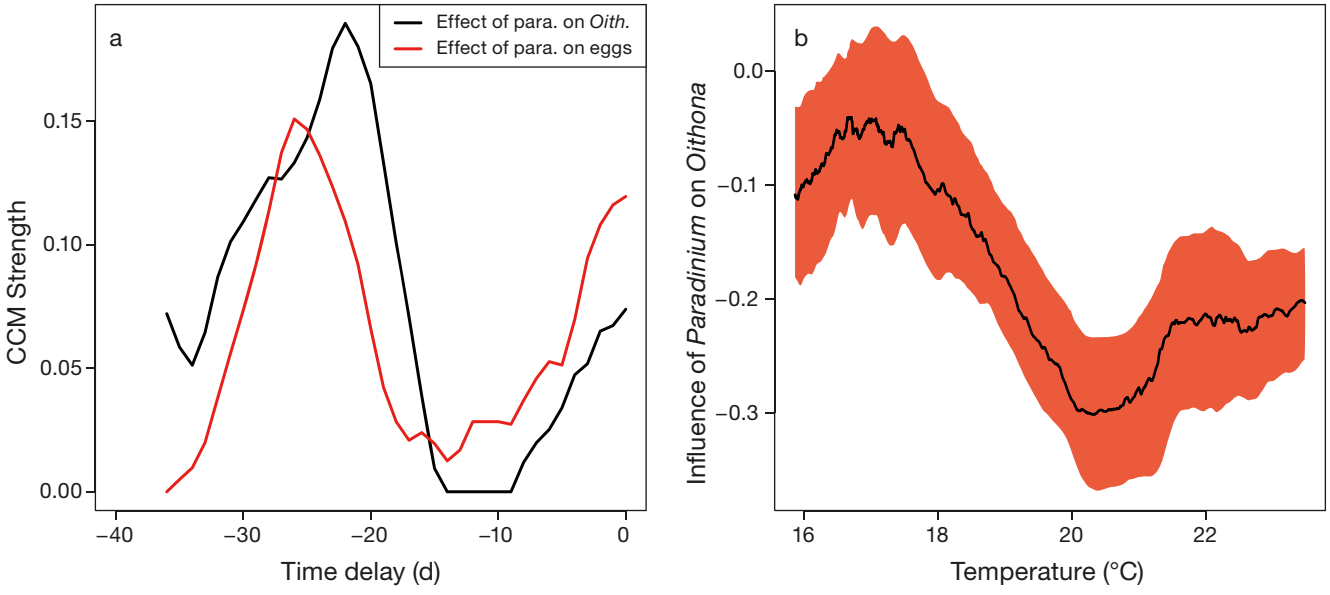

Fig. 3. Assessing the relationship between *Paradinium* spp. and *Oithona* spp. abundance. (a) Causal influence measured by convergent cross mapping (CCM) at different delays of the effect of *Paradinium* spp. on *Oithona* spp. abundance (black) and number of individuals carrying eggs (red). Note that *Paradinium* spp. has a peak interaction strength at ~23 d, roughly corresponding to the generation time of *Oithona* spp. (b) *S*-Map coefficients with random embeddings quantify the effect of the parasite on host abundance with a 23–26 d lag. Black line: generated by averaging across all embeddings; red region: standard deviation of the average in each window. Note that the strongest (negative) influences occur between 20 and 22°C

relative strength of the parasite on total *Oithona* spp. abundance was slightly stronger (higher peak CCM strength; Fig. 3a) than that on the subpopulation of adults carrying egg sacs at the 22–23 d time delay. Conversely, the instantaneous (delay = 0 d) effect of the parasite on the subpopulation of ovigerous females was much stronger than that of the parasite on the entire population.

Analysis of the *S*-map coefficients of the *Paradinium* spp. population's effect on *Oithona* spp. in multiple random embeddings suggests that the parasite almost always (89% of coefficients) had a negative influence on the host population (Fig. 3b). The relationship was temperature-dependent: the relative influence of the parasite was stronger in moderate local water temperatures (20–22°C) relative to colder (16–19°C) and very warm (>22°C) periods. This finding suggests that there is an optimal temperature range in which *Paradinium* spp. is most able to negatively impact the *Oithona* spp. population.

4. DISCUSSION

We combined 3 technologies — *in situ* microscopy, deep learning, and EDM — to identify a previously unobserved parasitic interaction in a densely sampled region, estimate prevalence over time based on *Paradinium*'s ephemeral end-stage gonosphere, and quantify the time scales of infection and host population control. Our analysis suggests a causal relationship between *Paradinium* spp. and its *Oithona* spp. host at a time scale of 22–23 d that is strongest when the water temperature is between 20 and 22°C. This temperature range is consistent with semiquantitative observations made by Skovgaard & Saiz (2006) of elevated *P. poucheti* prevalence during warm summer months (24–25°C) in the NW Mediterranean. There is otherwise little available data to quantify *Paradinium* spp. life cycle timing, environmental conditions favorable for the parasite's growth, or its effect on the overall host population.

EDM revealed several relevant time scales of the parasite's influence on ovigerous *Oithona* spp. and the overall host population: an instantaneous effect on egg-bearing individuals, a 22–23 d lag on the host population, and a 26 d delay on brood size. At a delay of 0 d, the parasite had a larger impact on the number of ovigerous females than on the whole population (Fig. 3a). We posit that this finding suggests that the observed *Paradinium* spp. is a parasitic castrator; the parasite consumes the ovaries during its internal life phase, reducing the number of visible egg-carrying individuals when there are many copepods exhibiting the ephemeral end-stage of the *Paradinium* spp. infection.

The longer delays can be attributed to the life-history of *Oithona* spp. The ~23 d delayed effect on the overall population aligns with reported generation times of *Oithona* (e.g. 19.7 d at 15°C, Sabatini & Kiørboe 1994; 23 d at 18°C, Huntley & Lopez 1992): if the parasite reduces the number of reproductive adults in the current population, the subsequent generation will have fewer adults. The slightly longer delay in the effect of the parasite on the number of ovigerous females suggests that it takes about 3 d for *Oithona* spp. to carry visually identifiable egg sacs once reaching the reproductive life stage (copepodite VI). Experimental data from other sources implies that *Oithona* spp. clutches hatch within 3–4 d in temperate waters like those at Scripps Pier (Nielsen et al. 2002).

Oithona spp. generation times (from egg to egg) have a noted temperature-dependence, ranging from 31–37 d at 15–17°C (Satapoomin et al. 2004) to approximately 1 wk in tropical waters at 25–30°C (Dvoretsky & Dvoretsky 2009). The Bělehrádek temperature function can be used to approximate the duration of each development stage of copepods (Corkett & McLaren 1979):

$$D = a(T - \alpha)^{-b} \quad (3)$$

where D is development time (in days), T is the temperature, and a, α, and b are fitted constants. Using constant values for each copepod life stage compiled by Eiane & Ohman (2004) and the temperature range measured by the SCCOOS array, we estimate *Oithona* spp. development time at the Scripps Pier to range between 8.6 and 32.5 d. The median temperature value in the study period was 18.2°C, suggesting a generation time of 15.7 d. These generation times are in keeping with the maximal effect of *Paradinium* spp. at 22–23 d: once the apparent parasite infection peaks in the image data, approximately one generation period elapses before the subsequent decline in the host is observed by the SPC.

These measured dynamics indicate that the parasite is endemic in the local *Oithona* spp. population, existing at low levels throughout the year of observation. We believe the observed host–parasite system was in equilibrium during the period of study, with the parasite regulating the *Oithona* spp. population size. This interpretation of our data is in accord with models of population control by parasitic infections, particularly that of Blower & Roughgarden (1987), who specifically considered the dynamics of a

marine host–parasitic castrator system. Their model suggested that such a system can exist in equilibrium when the disease agent is endemic and can enhance long-term host population stability as a process of co-diversification of the parasite and the host. The *Oithona–Paradinium* system we studied exhibits such behavior. The parasite's presence is inversely related to ovigerous females, indicating that *Paradinium* spp. inhibits the fecundity of the population at a time scale associated with the gestation period of *Oithona* spp.

While *Paradinium* spp. appears to be endemic and its relationship with *Oithona* spp. in equilibrium, without historical data we cannot definitively establish the state of the system. With only 1 yr of data, we cannot determine if the parasite is invasive or has historically been a part of the SCB plankton community. To our knowledge, *Paradinium* spp. has not previously been observed in the SCB despite decades of consistent study, perhaps due to the transient nature of the ectoparasitic gonosphere life stage. There is a wealth of local data that might be drawn upon to answer this question, particularly historic preserved net samples collected by the California Cooperative Oceanic Fisheries Investigations organization. Unfortunately, as previous studies have noted that chemical preservation techniques destroy *Paradinium* spp. after sporulation and attachment to the anal somite of the host's urosome, visual identification of the infection might not be possible from historic samples (Skovgaard & Saiz 2006). Counting endoparasites or conducting genomic analyses is an option but would require destruction of tissue (Bucklin & Allen 2004, Ruane & Austin 2017, Totoiu et al. 2020).

Previous studies have noted that parasitic infections of copepods in subpolar latitudes are temperature-dependent, suggesting that parasites are most pervasive in late summer and early autumn when the water is the warmest. Two parasitic dinoflagellates, *Atelodinium* spp. and *Blastiodinium* spp., have regularly been observed infecting copepods in warm coastal waters (Ianora et al. 1987, Skovgaard & Salomonsen 2009). Alves-de-Souza et al. (2011) found copepods infected with *Blastiodinium* spp. in oligotrophic Mediterranean waters and experimentally confirmed that elevated sporulation rates occur in warmer water.

Reports of *Paradinium* spp. are rare, likely due to the ephemeral nature of the external end-life stage. Observations have an apparent seasonality, with most samples being collected in the summer months (Skovgaard & Saiz 2006, Skovgaard & Daugbjerg 2008). Jepps (1937) suggested that the sporulation rate of a different, but potentially related, copepod parasite is temperature-dependent. This association with warmer temperatures is also a feature of the *Paradinium–Oithona* system. The *S*-map results suggest the parasite has the greatest effect on the *Oithona* spp. population during warm periods when the water temperature is between 20 and 22°C. This temperature zone perhaps represents a range in which the parasite can optimally complete its internal life stage while not overtaking *Oithona* spp. egg-production rates.

The effect of temperature aligns with the Blower & Roughgarden (1987) model of parasitic castration. For *Paradinium* spp. to have a regulatory effect on the host population, the net reproductive rate must be greater than the replacement rate of fertile copepods. The temperature range indicated by the *S*-map suggests that the parasite is better suited to reproduce in warm water. This finding reflects those of previous observations of *Paradinium* spp. and other parasites of metazoans.

The data we analyzed were collected during an extraordinarily warm period in the SCB due to the combined effect of the Blob and the equatorial El Niño 2015–2016. Marine heatwaves like the Blob, while uncommon by historic standards, are increasingly likely climatic events (Oliver et al. 2018). In the SCB, these events are associated with large temperature anomalies in the upper 100 m of the ocean, consistent with the ideal temperature range for *Paradinium* spp. becoming more common (Fumo et al. 2020). *Paradinium* control of copepod populations may become more broadly acute in the context of rising surface ocean temperatures.

Warmer waters have also been associated with elevated parasitic activity in a variety of marine organisms through increased host stress, pathogen virulence, pathogen range expansion, and host changes (Peacock et al. 2014, Cohen et al. 2018, Shields 2019). Other environmental changes associated with higher water temperature, such as acidification and increased salinity, can likewise intensify parasitic activity and pathology (Byers 2021). Consistent with these observations, there is mounting evidence of high abundances of parasitic organisms in all ocean basins, including at polar latitudes (Lima-Mendez et al. 2015). Conversely, 18S DNA sequencing studies in the Western Antarctic Peninsula found elevated protozoan parasite loads during cooler periods (Cleary & Durbin 2016). Together with our results, these studies suggest that fine temporal resolution sampling methods are needed to quantify how parasite–host relationships will change in the global ocean.

Our study revealed the consistent presence of a parasitic castrator in one of the most studied zooplankton populations in the world. The time series acquired by the *in situ* camera system revealed a dynamic link between the copepod population and the parasite. While the SPC can monitor populations, the instrument cannot track individuals in time and space nor, therefore, establish parasitic intensity or abundance. Moreover, we cannot determine the sex ratio of the population, quantify the numbers of copepods at different life stages, or make exact volumetric estimates of abundance from the image data. We thus stress that our interpretation of these data is based strictly on the counts generated from images classified by the CNN.

The CNN itself is a potential source of error and consternation. When one trains a supervised automated classifier, they are implicitly encoding a static mapping between input images and the desired output. The model's performance degrades when the statistics of the unlabeled target data differ from that of the training data (Moreno-Torres et al. 2012). Reasonable model performance on a random subset of training data does not guarantee accurate output on new data. The problem of so-called distribution shift is pervasive and of renewed interest in the machine learning community (Taori et al. 2020). We were careful to evaluate our model in new regions of time that might represent changing populations in different environmental circumstances. The analysis of FDR and FOR indicates that our CNN overestimated the classes of interest but likely missed a negligibly small number of relevant samples. We can thus be confident that we did not miss many relevant ROIs but must be cautious in our interpretation: the estimated prevalence of ovigerous and parasitized copepods reported in this study should be understood as a maximum. This underscores that any future work should explicitly consider a distribution shift in study design, perhaps by incorporating alternate approaches such as quantification (Gonzalez et al. 2019, Orenstein et al. 2020a).

Despite the limitations of this sampling methodology, the new type of data is extremely valuable for studying gross population-level effects via techniques like EDM that make limited assumptions about the study system. Laboratory experiments should be conducted to quantify individual effects of *Paradinium* spp. on *Oithona* spp., including the parasite's influence on host motility and behavior; changes in the host's growth and fecundity rates; and a precise estimate of the relative duration of the endo- and ectoparasitic phases of the *Paradinium* life cycle. Future field operations should couple *in situ* imaging systems with consistent co-located net or bottle samples. Direct access to biological material will facilitate genomic analyses and allow researchers to dissect hosts to establish infection rates. Together, these data streams would allow better quantification of the presence and effects of parasites on zooplankton populations. These data sets will help assess how parasites fit into food-web models, affect energy transfer in marine systems, and influence organic carbon fluxes.

Data availability. Human-annotated training data, human-corrected count data, and automated count data are available in UCSD Library Data Repository: https://doi.org/10.5281/zenodo.6502396

Acknowledgements. The authors thank Drs. Peter Franks and Jules Jaffe at UCSD for their support and invaluable advice at all stages of this project. The authors are also indebted to Dr. Jaime Gómez-Gutiérrez of the Instituto Politécnico Nacional de México for his critical reading and insightful comments on the manuscript. E.C.O was funded by the National Science Foundation BIGDATA Initiative (NSF IIS 15-46351). E.S. was funded under Department of Interior grant USDI-NPS P20AC00527. All machine learning experiments were performed on a GPU provided by the NVIDIA Corporation's Academic Hardware Donation Program.

LITERATURE CITED

Alves-de-Souza C, Cornet C, Nowaczyk A, Gasparini S, Skovgaard A, Guillou L (2011) *Blastodinium* spp. infect copepods in the ultra-oligotrophic marine waters of the Mediterranean Sea. Biogeosciences 8:2125–2136

Beardsley RC, Dever EP, Lentz SJ, Dean JP (1998) Surface heat flux variability over the northern California shelf. J Geophys Res Oceans 103:21553–21586

Benfield MC, Grosjean P, Culverhouse PF, Irigoien X and others (2007) RAPID: research on automated plankton identification. Oceanography (Wash DC) 20:172–187

Blower S, Roughgarden J (1987) Population dynamics and parasitic castration: a mathematical model. Am Nat 129: 730–754

Bograd SJ, Chereskin TK, Roemmich D (2001) Transport of mass, heat, salt, and nutrients in the southern California Current System: annual cycle and interannual variability. J Geophys Res Oceans 106:9255–9275

Bucklin A, Allen LD (2004) MtDNA sequencing from zooplankton after long-term preservation in buffered formalin. Mol Phylogenet Evol 30:879–882

Bush AO, Lafferty KD, Lotz JM, Shostak AW (1997) Parasitology meets ecology on its own terms: Margolis et al. revisited. J Parasitol 83: 575–583

Byers JE (2021) Marine parasites and disease in the era of global climate change. Annu Rev Mar Sci 13:397–420

Cavole LM, Demko AM, Diner RE, Giddings A and others (2016) Biological impacts of the 2013–2015 warm-water anomaly in the Northeast Pacific: winners, losers, and the future. Oceanography (Wash DC) 29:273–285

Chatton E (1910) *Paradinium paucheti*, ng, n. sp., flagellé parasite d'*Arcatia clausi* Giesbrecht (copépode pélagique). C R Seances Soc Biol Fil 69:341–342

Chatton E, Soyer M (1973) Le cycle évolutif du *Paradinium poucheti* Chatton, flagellé parasite plasmodial des copépodes. Les paradinides. Ann Sci Nat Zool 15:27–60

Cleary AC, Durbin EG (2016) Unexpected prevalence of parasite 18S rDNA sequences in winter among Antarctic marine protists. J Plankton Res 38:401–417

Cohen RE, James CC, Lee A, Martinelli MM and others (2018) Marine host–pathogen dynamics: influences of global climate change. Oceanography (Wash DC) 31: 182–193

Corkett CJ, McLaren IA (1979) The biology of *Pseudocalanus*. Adv Mar Biol 15:1–231

Deyle ER, May RM, Munch SB, Sugihara G (2016) Tracking and forecasting ecosystem interactions in real time. Proc R Soc B 283:20152258

Di Lorenzo E, Schneider N, Cobb KM, Franks PJS and others (2008) North Pacific Gyre Oscillation links ocean climate and ecosystem change. Geophys Res Lett 35: L08607

Dobson A, Lafferty KD, Kuris AM, Hechinger RF, Jetz W (2008) Homage to Linnaeus: How many parasites? How many hosts? Proc Natl Acad Sci USA 105:11482–11489

Dvoretsky VG, Dvoretsky AG (2009) Life cycle of *Oithona similis* (Copepoda: Cyclopoida) in Kola Bay (Barents Sea). Mar Biol 156:1433–1446

Eiane K, Ohman MD (2004) Stage-specific mortality of *Calanus finmarchicus*, *Pseudocalanus elongatus* and *Oithona similis* on Fladen Ground, North Sea, during a spring bloom. Mar Ecol Prog Ser 268:183–193

Fields DM, Runge JA, Thompson C, Shema SD and others (2015) Infection of the planktonic copepod *Calanus finmarchicus* by the parasitic dinoflagellate, *Blastodinium* spp: effects on grazing, respiration, fecundity and fecal pellet production. J Plankton Res 37:211–220

Fumo JT, Carter ML, Flick RE, Rasmussen LL, Rudnick DL, Iacobellis SF (2020) Contextualizing marine heatwaves in the Southern California Bight under anthropogenic climate change. J Geophys Res 125:e2019JC015674

Genovese C, Wasserman L (2002) Operating characteristics and extensions of the false discovery rate procedure. J R Stat Soc B 64:499–517

González P, Álvarez E, Díez J, López-Urrutia Á, del Coz JJ (2017) Validation methods for plankton image classification systems. Limnol Oceanogr Methods 15:221–237

González P, Castano A, Peacock EE, Díez J, Del Coz JJ, Sosik HM (2019) Automatic plankton quantification using deep features. J Plankton Res 41:449–463

Guidi L, Chaffron S, Bittner L, Eveillard D and others (2016) Plankton networks driving carbon export in the oligotrophic ocean. Nature 532:465–470

Harvell CD, Kim K, Burkholder JM, Colwell RR and others (1999) Emerging marine diseases — climate links and anthropogenic factors. Science 285:1505–1510

Ho J, Perkins PS (1985) Symbionts of marine Copepoda: an overview. Bull Mar Sci 37:586–598

Huntley ME, Lopez MD (1992) Temperature-dependent production of marine copepods: a global synthesis. Am Nat 140:201–242

Huyer A (1983) Coastal upwelling in the California Current system. Prog Oceanogr 12:259–284

Ianora A, Mazzocchi MG, Scotto di Carlo B (1987) Impact of parasitism and intersexuality on Mediterranean populations of *Paracalanus parvus* (Copepoda: Calanoida). Dis Aquat Org 3:29–36

Jacox MG, Hazen EL, Zaba KD, Rudnick DL, Edwards CA, Moore AM, Bograd SJ (2016) Impacts of the 2015–2016 El Niño on the California Current System: early assessment and comparison to past events. Geophys Res Lett 43:7072–7080

Jepps MW (1937) Memoirs: on the protozoan parasites of *Calanus finmarchicus* in the Clyde Sea area. J Cell Sci s2-79:589–658

Ji R, Stegert C, Davis CS (2013) Sensitivity of copepod populations to bottom-up and top-down forcing: a modeling study in the Gulf of Maine region. J Plankton Res 35:66–79

Johnson PTJ, Ives AR, Lathrop RC, Carpenter SR (2009) Long-term disease dynamics in lakes: causes and consequences of chytrid infections in *Daphnia* populations. Ecology 90:132–144

Kim HJ, Miller AJ, McGowan J, Carter ML (2009) Coastal phytoplankton blooms in the Southern California Bight. Prog Oceanogr 82:137–147

Kiørboe T (1997) Population regulation and role of mesozooplankton in shaping marine pelagic food webs. Hydrobiologia 363:13–27

Krizhevsky A, Sutskever I, Hinton GE (2012) ImageNet classification with deep convolutional neural networks. Adv Neural Inf Process Syst 25:1106–1114

Lafferty KD, Kuris AM (2009) Parasitic castration: the evolution and ecology of body snatchers. Trends Parasitol 25: 564–572

Lafferty KD, Dobson AP, Kuris AM (2006) Parasites dominate food web links. Proc Natl Acad Sci USA 103:11211–11216

LeCun Y, Bengio Y, Hinton G (2015) Deep learning. Nature 521:436–444

Legendre L, Rivkin RB (2002) Fluxes of carbon in the upper ocean: regulation by food-web control nodes. Mar Ecol Prog Ser 242:95–109

Lima-Mendez G, Faust K, Henry N, Decelle J and others (2015) Determinants of community structure in the global plankton interactome. Science 348:1262073

Lynn RJ, Bograd SJ (2002) Dynamic evolution of the 1997–1999 El Niño–La Niña cycle in the southern California Current System. Prog Oceanogr 54:59–75

MacLeod N, Benfield M, Culverhouse P (2010) Time to automate identification. Nature 467:154–155

Margolis L, Esch GW, Holmes JC, Kuris AM, Schad G (1982) The use of ecological terms in parasitology (report of an ad hoc committee of the American Society of Parasitologists). J Parasitol 68:131–133

McCallum HI, Kuris A, Harvell CD, Lafferty KD, Smith GW, Porter J (2004) Does terrestrial epidemiology apply to marine systems? Trends Ecol Evol 19:585–591

Moreno-Torres JG, Raeder T, Alaiz-Rodríguez R, Chawla NV, Herrera F (2012) A unifying view on dataset shift in classification. Pattern Recognit 45:521–530

Morgan SG, Shanks AL, MacMahan J, Reniers AJHM, Griesemer CD, Jarvis M, Fujimura AG (2017) Surf zones regulate larval supply and zooplankton subsidies to nearshore communities. Limnol Oceanogr 62:2811–2828

Nielsen TG, Møller EF, Satapoomin S, Ringuette M, Hopcroft RR (2002) Egg hatching rate of the cyclopoid copepod *Oithona similis* in arctic and temperate waters. Mar Ecol Prog Ser 236:301–306

Nishida S (1985) Taxonomy and distribution of the Family Oithonidae (Copepoda, Cyclopoida) in the Pacific and Indian Oceans. Bull Ocean Res Inst Univ Tokyo 20:1–167

Ohman MD (1986) Predator-limited population growth of the copepod *Pseudocalanus* sp. J Plankton Res 8:673–713

Oliver EC, Donat MG, Burrows MT, Moore PJ and others (2018) Longer and more frequent marine heatwaves over the past century. Nat Commun 9:1324

Orenstein EC, Beijbom O (2017) Transfer learning and deep feature extraction for planktonic image data sets. In: 2017 IEEE winter conference on applications of computer vision (WACV), 24–31 March 2017, Santa Rosa, CA. IEEE, Piscataway, NJ, p 1082–1088

Orenstein EC, Kenitz KM, Roberts PLD, Franks PJS, Jaffe JS, Barton AD (2020a) Semi- and fully supervised quantification techniques to improve population estimates from machine classifiers. Limnol Oceanogr Methods 18: 739–753

Orenstein EC, Ratelle D, Briseño-Avena C, Carter ML, Franks PJS, Jaffe JS, Roberts PLD (2020b) The Scripps Plankton Camera system: a framework and platform for *in situ* microscopy. Limnol Oceanogr Methods 18:681–695

Peacock EE, Olson RJ, Sosik HM (2014) Parasitic infection of the diatom *Guinardia delicatula*, a recurrent and ecologically important phenomenon on the New England Shelf. Mar Ecol Prog Ser 503:1–10

Pineda J (1991) Predictable upwelling and the shoreward transport of planktonic larvae by internal tidal bores. Science 253:548–549

Ruane S, Austin CC (2017) Phylogenomics using formalin-fixed and 100+ year-old intractable natural history specimens. Mol Ecol Resour 17:1003–1008

Sabatini M, Kiørboe T (1994) Egg production, growth and development of the cyclopoid copepod *Oithona similis*. J Plankton Res 16:1329–1351

Saberski E, Bock AK, Goodridge R, Agarwal V, Lorimer T, Rifkin SA, Sugihara G (2021) Networks of causal linkage between eigenmodes characterize behavioral dynamics of *Caenorhabditis elegans*. PLOS Comput Biol 17:e1009329

Satapoomin S, Nielsen TG, Hansen PJ (2004) Andaman Sea copepods: spatio-temporal variations in biomass and production, and role in the pelagic food web. Mar Ecol Prog Ser 274:99–122

Shields JD (1994) The parasitic dinoflagellates of marine crustaceans. Annu Rev Fish Dis 4:241–271

Shields JD (2017) Collection techniques for the analyses of pathogens in crustaceans. J Crustac Biol 37:753–763

Shields JD (2019) Climate change enhances disease processes in crustaceans: case studies in lobsters, crabs, and shrimps. J Crustac Biol 39:673–683

Sinnett G, Feddersen F, Lucas AJ, Pawlak G, Terrill E (2018) Observations of nonlinear internal wave run-up to the surfzone. J Phys Oceanogr 48:531–554

Skovgaard A (2014) Dirty tricks in the plankton: diversity and role of marine parasitic protists. Acta Protozool 53:51–62

Skovgaard A, Daugbjerg N (2008) Identity and systematic position of *Paradinium poucheti* and other *Paradinium*-like parasites of marine copepods based on morphology and nuclear-encoded SSU rDNA. Protist 159: 401–413

Skovgaard A, Saiz E (2006) Seasonal occurrence and role of protistan parasites in coastal marine zooplankton. Mar Ecol Prog Ser 327:37–49

Skovgaard A, Salomonsen XM (2009) *Blastodinium galatheanum* sp. nov. (Dinophyceae) a parasite of the planktonic copepod *Acartia negligens* (Crustacea, Calanoida) in the central Atlantic Ocean. Eur J Phycol 44:425–438

Sommer U, Adrian R, De Senerpont Domis L, Elser JJ and others (2012) Beyond the Plankton Ecology Group (PEG) model: mechanisms driving plankton succession. Annu Rev Ecol Evol Syst 43:429–448

Storey JD (2003) The positive false discovery rate: a Bayesian interpretation and the *q*-value. Ann Stat 31:2013–2035

Sugihara G (1994) Nonlinear forecasting for the classification of natural time series. Philos Trans R Soc A 348:477–495

Sugihara G, May R, Ye H, Hsieh C, Deyle E, Fogarty M, Munch S (2012) Detecting causality in complex ecosystems. Science 338:496–500

Taori R, Dave A, Shankar V, Carlini N, Recht B, Schmidt L (2020) Measuring robustness to natural distribution shifts in image classification. Adv Neural Inf Process Syst 33: 18583–18599

Théodoridès J (1989) Parasitology of marine zooplankton. Adv Mar Biol 25:117–177

Totoiu CA, Phillips JM, Reese AT, Majumdar S, Girguis PR, Raston CL, Weiss GA (2020) Vortex fluidics-mediated DNA rescue from formalin-fixed museum specimens. PLOS ONE 15:e0225807

Turner JT (2004) The importance of small planktonic copepods and their roles in pelagic marine food webs. Zool Stud 43:255–266

Ushio M, Hsieh C, Masuda R, Deyle ER and others (2018) Fluctuating interaction network and time-varying stability of a natural fish community. Nature 554:360–363

Verity PG, Smetacek V (1996) Organism life cycles, predation, and the structure of marine pelagic ecosystems. Mar Ecol Prog Ser 130:277–293

Ward GM, Neuhauser S, Groben R, Ciaghi S, Berney C, Romac S, Bass D (2018) Environmental sequencing fills the gap between parasitic haplosporidians and free-living giant amoebae. J Eukaryot Microbiol 65:574–586

Worden AZ (2006) Picoeukaryote diversity in coastal waters of the Pacific Ocean. Aquat Microb Ecol 43:165–175

Ye H, Deyle ER, Gilarranz LJ, Sugihara G (2015) Distinguishing time-delayed causal interactions using convergent cross mapping. Sci Rep 5:14750

Yosinski J, Clune J, Bengio Y, Lipson H (2014) How transferable are features in deep neural networks? Adv Neural Inf Process Syst 27:3320–3328

Zaba KD, Rudnick DL (2016) The 2014–2015 warming anomaly in the Southern California Current System observed by underwater gliders. Geophys Res Lett 43: 1241–1248

Editorial responsibility: Marsh Youngbluth, Fort Pierce, Florida, USA
Reviewed by: P. Gonzalez and 3 anonymous referees

Submitted: October 9, 2021
Accepted: April 27, 2022
Proofs received from author(s): June 8, 2022